TABLE 1: Clinical and Laboratory Findings at Muscle Biopsy or DNA Analysis

Patient	Age at Muscle Biopsy (mo)	Sex	Clinical Diagnosis before Muscle Biopsy	Main Complaints	High Arched Palate	Laboratory Findings			Muscle Pathology							Respiratory Chain Enzyme Activities								
						Serum CK (U/L) (n = 180)	Blood lactate (mg/ml) (n = 5–20)	CSF lactate (mg/ml) (n = 5–15)	RRF	SSV	COX Deficiency					Complex I		Complex II		Complex III		Complex IV		CS
											RRF	non-RRF Type 1	Small Artery	Muscle Spindle	Nerve	/mg Protein (%)	/CS (%)	/mg Protein (%)	/CS (%)	/mg Protein (%)	/CS (%)	/mg Protein (%)	/CS (%)	/mg Protein (%)
1	8	F	CMP	Muscle weakness	–	ND	12.5	8.3	+	–	All	+	–	NP	NP	ND	ND	ND	ND	ND	ND	ND	ND	ND
2	5	F	CMP	Poor sucking	+	226	24	ND	+	–	All	+	–	NP	–	ND	ND	ND	ND	ND	ND	ND	ND	ND
3	5	F	MMP	Failure to thrive	?	422	25.2	21.3	+	–	All	+	–	NP	–	105.7	50.2	106.6	52.5	108.8	52.5	44.6	23.1	193.2
4	3	F	MMP	Failure to thrive	–	203	149.3	50	+	±	All	+	–	NP	NP	72.4	39.7	145.6	82.7	118.6	66	54.1	32.3	167.5
5	4	M	MMP	Failure to thrive	–	604	23.5	11.1	+	–	All	+	–	–	–	ND	ND	ND	ND	ND	ND	ND	ND	ND
6	9	M	CMD	Floppy infant	+	644	18.7	ND	+	–	All	+	–	–	–	68.5	39.1	125.6	74.4	124	71.9	63.7	39.7	160.7
7	ND	F	MMP	Poor sucking	?	279	81.1	ND	ND	ND	ND	ND	ND	ND	ND	ND	ND	ND	ND	ND	ND	ND	ND	ND
8	ND	M	MMP	Floppy infant	?	182	24.4	ND	ND	ND	ND	ND	ND	ND	ND	ND	ND	ND	ND	ND	ND	ND	ND	ND

F/M = female/male; CMD = congenital muscular dystrophy; CMP = congenital myopathy; COX = cytochrome c oxidase; MMP = mitochondrial myopathy; ND = not determined; NP = not present in sections; RRF = ragged-red fiber; SSV = strongly succinate-dehydrogenase–reactive blood vessels.

TABLE 2: Developmental Milestones and Clinical Course

Patient	Age at Last Investigation	Head Control	Walked Alone	Muscle Weakness	Gavage Feeding (age)	Respirator (age)	CK, Lactate Data	Complications
1	15 yr	Unknown	2 yr 0 mo	(–)	(–)	(–)	ND	None
2	11 yr	8 mo	2 yr 8 mo	(–)	3–4 mo	(–)	Normal after 3 yr; transient mild elevated serum CK and lactate during infection	None
3	11 yr	Unknown (roll over 9 mo)	Late infancy	Mild exercise intolerance (walking for long time or climbing)	(–)	(–)	ND	None
4	5 yr	9 mo	1 yr 3 mo	(–)	(–)	2–6 mo	Normal at the age of 1 yr 10 mo	None
5	6 yr	10 mo	12 mo	(–)	0–2 d	(–)	ND	Febrile convulsion (2 yr)
6	1 yr 6 mo	9 mo	1 yr 6 mo	Mild muscle weakness	(–)	(–)	Normal after 11 mo	None
7	4 yr	8–9 mo	1 yr 4 mo	(–)	(–)	(–)	Normal after 2 yr 11 mo	None
8	3 yr	7 mo	1 yr 4 mo	(–)	(–)	(–)	Normal after 2 yr	None

CK = creatinine kinase; ND = not determined.

Results

Clinical Features

Profound generalized muscle hypotonia and weakness occurred between birth and 3 months of age. Involvement of facial muscles with a high-arched palate was noted in 2 patients (see Table 1). The clinical diagnoses prior to muscle biopsy were mitochondrial myopathy in 5 patients, congenital myopathy in 2, and congenital muscular dystrophy in 1.

Review of clinical course after muscle biopsy or DNA analysis (Table 2) showed that all patients, except patient 6, recovered to an almost normal state during the 3-year follow-up period. Patients 2 and 5 required tube feeding during early infancy, and patient 4 was on a respirator from 2 to 6 months of age. All learned to walk by 1–2 years of age and could run normally when they were last examined. Although patient 6 had a slight delay in gross motor developmental milestones at 18 months of age, he could walk without support. No patient had short stature, renal dysfunction, liver dysfunction, cardiomyopathy, or diabetes mellitus.

Laboratory Findings

Blood lactate levels were normal in 2 patients, slightly elevated (20–25 mg/dl) in 4, and more than twice the

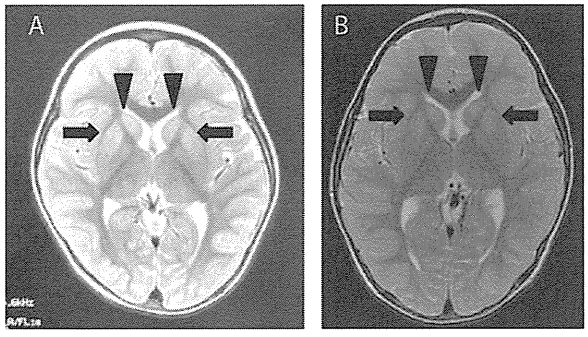

FIGURE 1: Brain MRI images of (A) patient 7 at the age of 23 months and (B) patient 8 at the age of 33 months. Abnormally high T2-weighted signals in bilateral caudate nuclei *(arrowheads)* and putamina *(arrows)*.

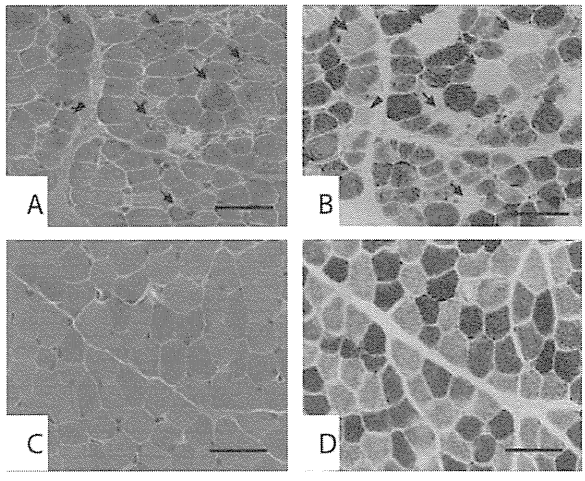

FIGURE 2: Representative muscle pathology. Patient 6 (A, B) and age-related control (aged 1 year and 3 months) without mitochondrial disease (C, D). Serial sections are stained with modified (A, C) Gomori trichrome and (B, D) COX stains. The muscle of the patient had marked fiber-size variation and numerous basophilic RRFs. RRFs *(arrows)* are always COX-deficient, and the fibers of normal appearance *(arrowheads)* are sometimes COX-deficient. Bar = 50μm.

normal level in 2 (see Table 1). Patient 4 had high blood and CSF lactate levels during early infancy, but the levels subsequently normalized. Serum CK levels during infancy were elevated in all patients (range, 182–644 U/L; mean, 366 U/L) and reached normal levels with development. In patients 7 and 8, brain magnetic resonance imaging (MRI) images revealed abnormally high T2-weighted signals in bilateral caudate nuclei and putamina at the age of 23 months (Fig 1A) and 33 months (see Fig 1B), respectively, although these signals had been previously normal at the age of 7 months and 13 months, respectively. Brain CT and MRI images performed in 2 other patients were normal.

Muscle Pathology

All biopsy specimens showed marked variation in fiber size. There were numerous ragged-red fibers (RRFs) in all specimens, comprising 5% to 25% of fibers (Fig 2A). RRFs frequently had oil-red O-positive vacuoles and stained strongly on periodic acid-Schiff (PAS). There was no obvious strongly SDH-reactive blood vessel and no abnormal blood vessel under light microscopy.[31] In all specimens, scattered muscle fibers were faintly positive to normal COX activity with focal deficiency (see Fig 2B). RRFs were always COX-negative. In several specimens, a portion of normal-appearing type 1 fibers (non-RRF) also showed reduced activity (see Fig 2A, B). COX activity of intrafusal fibers, small arteries, and intramuscular peripheral nerves appeared normal (see Table 1).

mtDNA Analysis

No large-scale mtDNA rearrangements were detected by long PCR and Southern methods. Total mtDNA

TABLE 3: Total Sequence Analysis of mtDNA

Gene/Patient	ND1	ND1	COI	ATP8	ATP8	ND4	$tRNA^{Glu}$	$tRNA^{Glu}$	D-loop
1								T14674G	C16197T
2	C3408T					C14067T	T14674C		
3				C8409T	A8459G			T14674G	
4							T14674C		
5		G3496T	T6185C				T14674C		
6							T14674C		
7							T14674C		
8							T14674C		

Fifteen polymorphisms were revealed that were not detected in 100 normal subjects. We identified homoplasmic mutations at np 14674 in the mitochondrial $tRNA^{Glu}$ in all 8 subjects. Patients 1 and 3 had the T14674G mutation and patients 2, 4, 5, 6, 7, and 8 had the T14674C mutation, neither of these mutations were detected in 200 normal controls.

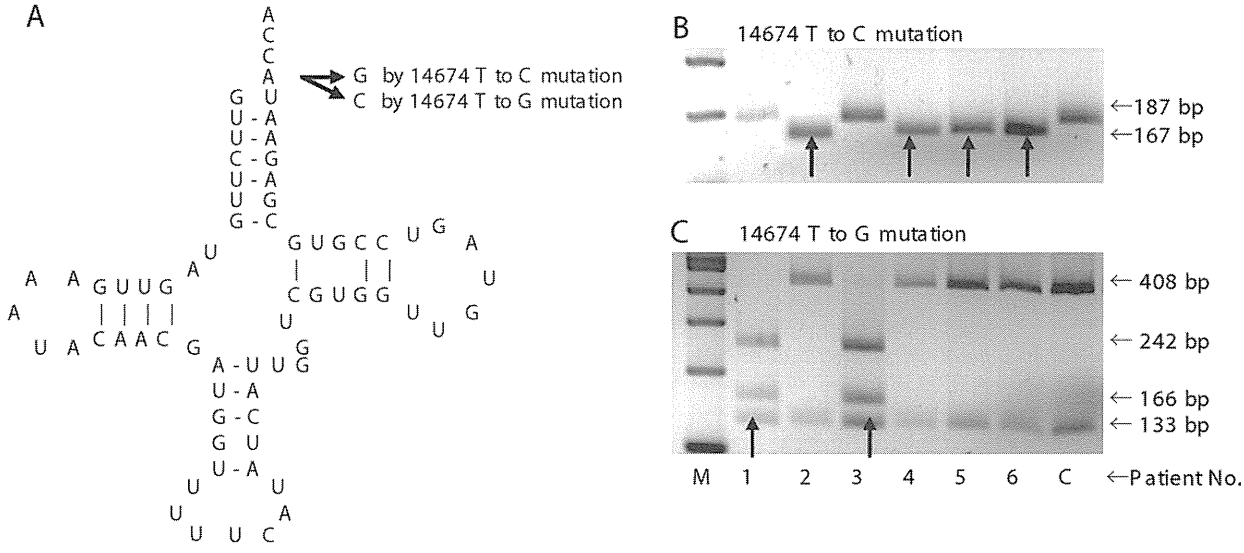

FIGURE 3: (A) Mutations at the discriminator base of tRNA^{Glu}. Nucleotide position 14674 is the discriminator identified by the aminoacyl-tRNA synthetase. The arrows show the A to G mutation by m.14674T>C and the A to C mutation by m.14674T>G. The CCA sequence is added to the nucleotide before this tRNA charges glutamate. (B) Identification of m.14674T>C mutation in mtDNA. The 187-bp PCR fragments with the mismatched and reverse primers were digested by *BclI*. Wild-type mtDNAs are indicated by 187-bp bands and mutant mtDNAs are indicated by 167-bp bands in patients 2, 4, 5, and 6 *(arrows)*. (C) Identification of m.14674T>G mutation in mtDNA. The amplified 541-bp PCR fragments were digested by *NlaIII*. Wild-type mtDNAs are indicated by cleaved fragments of 408bp and 133bp, and mutant mtDNAs are indicated by 133-bp, 242-bp, and 166-bp bands divided from the 408-bp bands in patients 1 and 3 *(arrows)*. Each fragment was detected on a 4% agarose gel and visualized with ethidium bromide under UV light.

sequencing from these patients revealed many polymorphisms. Most were silent mutations or reported as normal polymorphisms according to a human mitochondrial genome database (MITOMAP).

Fifteen base changes were not present in 100 normal Japanese adults (Table 3). In the reported polymorphisms, patients 2, 4, 5, 6, 7, and 8 had previously reported T to C base change at np 14674 in the tRNA^{Glu}. Furthermore, patients 1 and 3 had a T to G base change at the same np (np 14674) in the mitochondrial tRNA^{Glu} gene, which has not been previously reported according to the MITOMAP database (Fig 3A). These base changes were confirmed by RFLP analysis and revealed to be homoplasmic (see Fig 3B, C; data for patients 7 and 8 not shown).

Mitochondrial tRNA Analysis

In northern blot analysis using total RNA extracted from muscle specimens of patients and normal infants, values were normalized by the amount of mitochondrial tRNA-Leu (UUR) and nuclear-encoded 5S rRNA as internal standards. The tRNA^{Glu} molecules in patients were the same size as those in normal infants. However, the amount of tRNA^{Glu} in patients was about one-fourth of that in normal controls. The amount of tRNA-Leu (UUR) in patients and normal infants remained unchanged (Fig 4).

By acid PAGE, the degrees of delay in electrophoresis of cybrids or naive myoblasts derived from patient 6 were identical to those of normal control 143B/TK-cells (Supporting Information Fig S1). This finding suggested that aminoacylation of tRNA^{Glu} from patients carrying the mutation was normal and glutamate was correctly charged to tRNA.

Biochemical Studies

Respiratory chain enzyme assay of skeletal muscle showed that complex IV activity in patients 3, 4, and 6 and

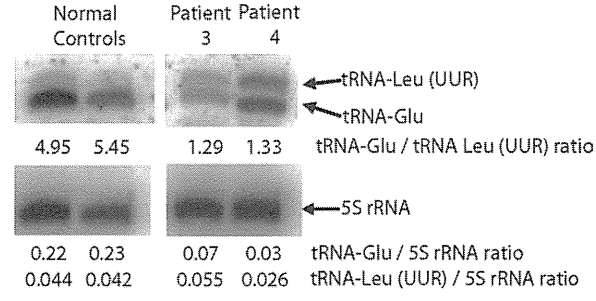

FIGURE 4: Quantitative analysis of tRNA^{Glu} in muscle. Total RNA was extracted from patients 3 and 4 as well as from the muscle specimen of 2 normal infants (normal controls). The same amount of each RNA sample was electrophoresed followed by northern hybridization. The amounts of tRNA^{Glu} were normalized by the amount of mitochondrial tRNA-Leu (UUR) and nuclear-encoded 5S ribosomal RNA. The amount of tRNA^{Glu} in patients was about one-fourth that in normal controls, although the amount of tRNA-Leu (UUR) remained unchanged in both patients and normal infants.

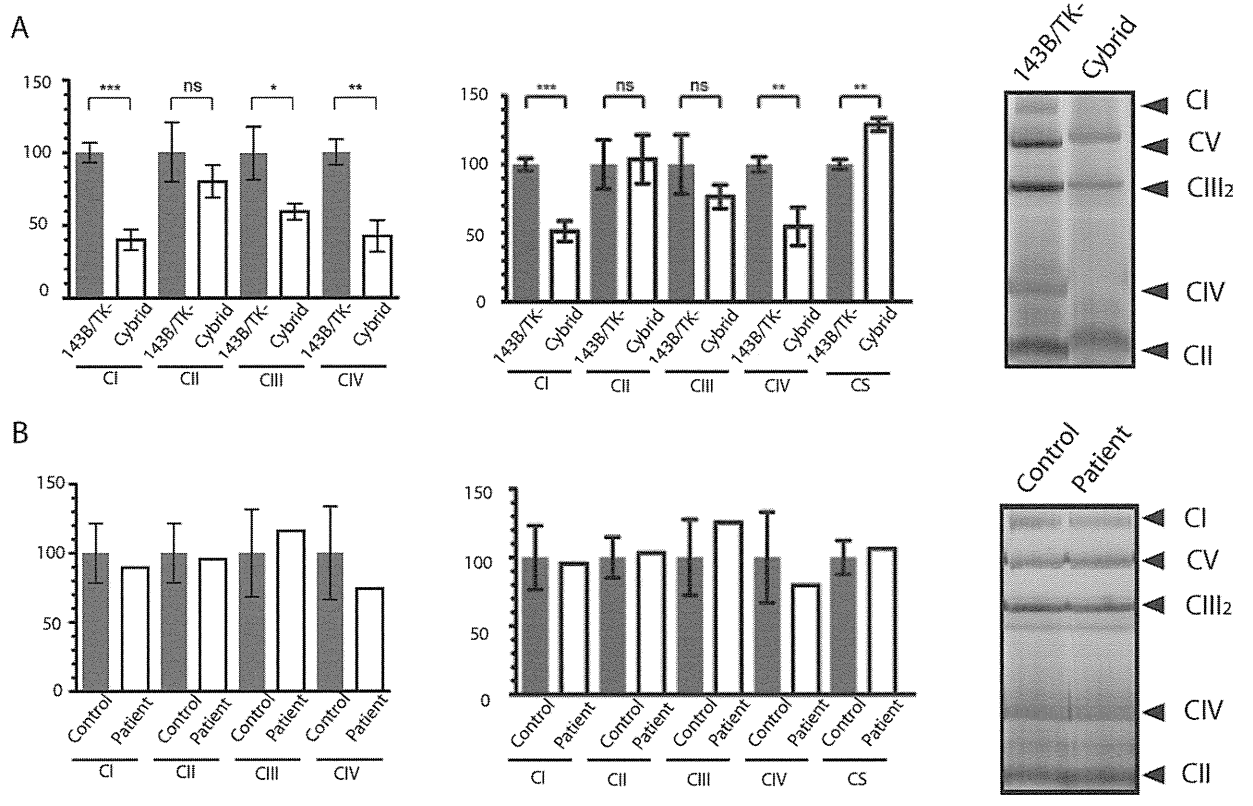

FIGURE 5: Respiratory chain enzyme assay and BN-PAGE of (A) cybrids derived from patient 6 compared with 143B/TK-cells and (B) naive myoblasts derived from patient 6 compared with normal control myoblasts. Enzyme activities are expressed as percent of mean normal control activity relative to protein and CS. Cybrids showed reduced levels of complexes I, III, and IV relative to protein and reduced levels of complexes I and IV relative to CS. BN-PAGE also revealed a severe decrease in the amount of complexes I and IV. Naive myoblasts of patient 6 showed normal respiratory chain enzyme activities and normal amounts of respiratory complex enzymes in BN-PAGE. BN-PAGE = blue native polyacrylamide gel electrophoresis; CS = citrate synthase.

complex I activity in patients 4 and 6 apparently decreased (see Table 1). The activities of complexes II and III relative to protein were within normal limits, while those relative to citrate decreased because CS activity increased.

To confirm the pathogenicity of the m.14674T>C mutation, respiratory chain enzyme assay and BN-PAGE were performed on mitochondrial proteins isolated from cybrids derived from patient 6 and 143B/TK-cells. In respiratory chain enzyme assay, cybrids showed reduced levels of complexes I, III, and IV relative to protein and reduced levels of complexes I and IV relative to CS compared with 143B/TK-cells. BN-PAGE also revealed a severe decrease in the amounts of complexes I and IV (Fig 5A). In contrast, the naive myoblasts of patient 6 showed normal respiratory chain enzyme activities and normal amounts of the respiratory complex enzymes in BN-PAGE (see Fig 5B).

Discussion

We examined 8 cases in 7 independent Japanese families with the reversible clinical phenotype of mitochondrial disorder, which is consistent with "benign COX deficiency myopathy." Recently, homoplasmic m.14674T>C mutation was reported in 17 affected individuals; the authors emphasized the importance of genetic testing to identify infants with this mitochondrial myopathy and predict a good prognosis.[21] In the present study, we identified the mutation in 6 patients. Identification of the same mutation in many Japanese patients supports the premise that detecting the mutation is useful in diagnosing the disease. Muscle specimens from all patients showed typical morphological features of mitochondrial myopathies in accordance with the classical fatal infantile form of COX deficiency, which is phenotypically similar to the benign form at an early stage. Therefore, detection of homoplasmic mutations in blood samples is important and useful for diagnosis of the benign form. In fact, we were able to make a diagnosis and predict a good prognosis for patients 7 and 8 based on mtDNA analyses using blood samples without muscle biopsy. Furthermore, in patients 1 and 3, we identified a novel homoplasmic m.14674T>G mutation. Clinical phenotypes were the same as those of patients carrying the m.14674T>C

mutation, providing further evidence that the mutation at this np is important to disease causation, and not only m.14674T>C but also m.14674T>G mutation should be tested for when clinicians suspect the disease.

In the literature, at least 19 patients have been reported as having "benign COX deficiency myopathy" or a similar disease.[2,15–21,32] Most of these patients showed clinical symptoms in only skeletal muscle and good recovery, which was similar to patients in this and a previous study.[21] However, with regard to the patient reported by Suzuki et al.,[19] who could not stand up at age 22 months and was probably mentally retarded, the tempo of recovery and subsequent disease outcome in such a patient is variable, and thus, the definition of the disease has been unclear. Lack of good recovery may be indicative of other diseases. Detection of m.14674T>C and m.14674T>G mutations should be helpful for redefinition of this disease. We also identified 2 siblings carrying the mutation with bilateral lesions in caudate nuclei and putamina, which are often affected in mitochondrial disorders such as Leigh encephalopathy. Abnormalities outside of muscle may have been overlooked in this disease. Thus we must draw attention not only to muscle, but also to the central nervous system, even at later stages of the disease.

Because the base changes are located at the end of the aminoacyl acceptor stem of $tRNA^{Glu}$, which plays an important role in tRNA identity as the discriminator base,[33] abnormality of the amino acid charge to tRNA molecule may occur. However, acid PAGE revealed that the aminoacylation ratio of $tRNA^{Glu}$ from a patient carrying the mutation was normal. Therefore, the mutation had no influence on the steady-state level of aminoacylation. However, the muscle specimen from patient 4 carrying the m.14674T>C mutation had 75% less $tRNA^{Glu}$ molecules than specimens from normal infants as previously reported.[21] Furthermore, $tRNA^{Glu}$ molecules of the muscle specimen from patient 3 carrying the m.14674T>G mutation also markedly decreased. Instability and reduction of tRNA molecule carrying a mutation in the corresponding tRNA gene of mtDNA may be responsible for mitochondrial diseases.[34,35] A reduction in the amount of $tRNA^{Glu}$ should be essential to affect translation. COX is a complex enzyme composed of 13 subunits. The 3 larger subunits (I, II, and III) are synthesized in the mitochondria under the direction of mtDNA using the mitochondrial tRNA molecules. It is possible that mtDNA mutation in the mitochondrial $tRNA^{Glu}$ has an influence on the synthesis of 1 of these 3 subunits by reduction of $tRNA^{Glu}$. In particular, subunit II (COXII) gene contains as many as 11 glutamates that constitute 4.8% of total amino acids in COXII, whereas glutamate constitutes 1.9% in the subunit I (COXI) gene and 2.7% in the subunit III (COXIII) gene. It has been reported that fatal infantile COX deficiency was characterized by the selective absence of subunits VIIa+VIIb under the control of nuclear DNA, whereas subunits VIIa+VIIb and COXII encoded by mtDNA in a benign type were absent.[36] The mutation in $tRNA^{Glu}$ gene may cause pathological findings by a translational depression of COXII-containing glutamates in highest proportion among the subunits. These facts indirectly support the pathogenicity of the mutation.

Biochemical analyses in this study revealed some new aspects of this disease. In respiratory chain enzyme assay of skeletal muscle, not only complex IV activity but also complex I activity significantly decreased. It is reasonable to suppose that a reduction in the amount of $tRNA^{Glu}$ should affect translation of not only complex IV but also other respiratory complexes. The activities of complexes II and III relative to CS also decreased because CS activity apparently increased, which suggested that the increase in the number of mitochondria was caused by respiratory enzyme deficiency. Both respiratory chain enzyme assay and BN-PAGE showed defects in complexes I and IV during biochemical studies using cybrids carrying m.14674T>C mutation. This finding directly revealed the pathogenicity of the mutation. Interestingly, naive myoblasts carrying the same mutation showed normal respiratory chain enzyme activities and normal amounts of the respiratory complex enzymes in BN-PAGE. From these facts, it is reasonable to think that nuclear factor(s) may compensate for the defects caused by mtDNA mutation in naive myoblasts through cell division and proliferation during the establishment of the myoblast cell line. The discrepancy between skeletal muscle specimen and myoblasts suggests that the recovery of the respiratory chain enzymes in the skeletal muscle in vivo and clinical symptoms was acquired through the cell proliferation and/or differentiation of myoblasts during the aging or development of the patients. In skeletal muscle in vivo, it is likely that enzyme defects and clinical symptoms become obvious during the early infantile period when compensation is insufficient. Unknown nuclear factor(s) relating to the control of the amount of $tRNA^{Glu}$ may be a key factor in mechanisms of recovery.

Because human mtDNA is maternally inherited, similar abnormalities should be seen in mother and siblings; however, most of the maternal families are asymptomatic. In our case, the mother of patient 6, who did not have a remarkable past history, also carried the m.14674T>C mutation. It seems appropriate to think

that maternal families who have nuclear factors compensating for the defects of the respiratory chain enzymes caused by mtDNA mutation become asymptomatic. In the cases with insufficient compensation, clinical presentations involving not only muscle but also central nervous system may appear, which is similar to our affected siblings.

In summary, we confirmed the pathogenicity of the mutation at np 14674 in $tRNA^{Glu}$ resulting in deficiency of multiple respiratory enzymes. We hypothesize that mtDNA mutation has a great impact on multiple respiratory chain enzyme activities and there should be compensatory mechanisms of nuclear factor(s). According to the degree of compensation, clinical features may vary from asymptomatic maternal families to patients with central nervous system involvement. Our results provide new insights into the disease known as "benign COX deficiency myopathy." We propose that this disease should be renamed "infantile reversible respiratory chain deficiency" as it is caused by deficiency of multiple respiratory chain enzymes, which may result in involvement beyond skeletal muscles.

Acknowledgments

This work was supported by a grant for Nervous and Mental Disorders from the Ministry of Health, Labour, and Welfare of Japan (15B-4 and 18A-5 to Y.G.); a Grant-in-Aid for Young Scientists (B) from the Ministry of Education, Culture, Sports, Science and Technology (17790738 to M.M.); and a grant from the Comprehensive Research Project on Health Sciences Focusing on Drug Innovation from the Japan Health Sciences Foundation (KHD2207 to Y.G.).

We thank the following attending physicians (all of whom were based in Japan) for referring their patients to us and responding to our follow-up questionnaires: Dr. H. Sasaki (Department of Pediatrics, Kurashiki Central Hospital, Kurashiki, Okayama), Dr. T. Segawa (Department of Pediatrics, Fuji Central Municipal Hospital, Fuji, Shizuoka), Dr. T. Miyajima (Department of Pediatrics, Tokyo Medical University, Shinjuku-ku, Tokyo), Dr. S. Mizukami (Department of Pediatrics, Hakodate Central Hospital, Hakodate, Hokkaido), Dr. H. Koide (Department of Pediatrics, Saitama Medical School Hospital, Saitama), and Dr. Y. Otsuka (Department of Pediatrics, Juntendo University Hospital, Bunkyo-ku, Tokyo).

Potential Conflict of Interest

Nothing to report.

References

1. Robinson BH. Human cytochrome oxidase deficiency. Pediatr Res 2000;48:581–585.
2. DiMauro S, Lombes A, Nakase H, et al. Cytochrome c oxidase deficiency. Pediatr Res 1990;28:536–541.
3. Nonaka I, Koga Y, Shikura K, et al. Muscle pathology in cytochrome c oxidase deficiency. Acta Neuropathol (Berl) 1988;77:152–160.
4. Shoubridge EA. Cytochrome c oxidase deficiency. Am J Med Genet 2001;106:46–52.
5. Sacconi S, Salviati L, Sue CM, et al. Mutation screening in patients with isolated cytochrome c oxidase deficiency. Pediatr Res 2003; 53:224–230.
6. Böhm M, Pronicka E, Karczmarewicz E, et al. Retrospective, multicentric study of 180 children with cytochrome c oxidase deficiency. Pediatr Res 2006;59:21–26.
7. Valnot I, Osmond S, Gigarel N, et al. Mutations of the SCO1 gene in mitochondrial cytochrome c oxidase (COX) deficiency with neonatal-onset hepatic failure and encephalopathy. Am J Hum Genet 2000;67:1104–1109.
8. Papadopoulou LC, Sue CM, Davidson MM, et al. Fatal infantile cardioencephalomyopathy with COX deficiency and mutations in SCO2, a COX assembly gene. Nat Genet 1999;23:333–337.
9. Valnot I, von Kleist-Retzow JC, Barrientos A, et al. A mutation in the human heme A: farnesyl transferase gene (COX10) causes cytochrome c oxidase deficiency. Hum Mol Genet 2000;9:1245–1249.
10. Antonicka H, Mattman A, Carlson CG, et al. Mutation in COX15 produce a defect in the mitochondrial heme biosynthetic pathway, causing early-onset fatal hypertrophic cardiomyopathy. Am J Hum Genet 2003;72:101–114.
11. Moraes CT, Shanske S, Tritschler H-J, et al. mtDNA depletion with variable tissue expression: a novel genetic abnormality in mitochondrial diseases. Am J Hum Genet 1991;48:492–501.
12. Mazziotta MRM, Ricci E, Bertini E, et al. Fatal infantile liver failure associated with mitochondrial DNA depletion. J Pediatr 1992;121: 896–901.
13. Oldfors A, Sommerland H, Holme E, et al. Cytochrome c oxidase deficiency in infancy. Acta Neuropathol (Berl) 1989;77:267–275.
14. Van Biervliet JP, Bruinvis L, Ketting D, et al. Hereditary mitochondrial myopathy with lactic acidemia, a De Toni-Fanconi-Debré syndrome, and a defective respiratory chain in voluntary striated muscles. Pediatr Res 1977;11:1088–1093.
15. DiMauro S, Nicholson JF, Hays AP, et al. Benign infantile mitochondrial myopathy due to reversible cytochrome c oxidase deficiency. Ann Neurol 1983;14:226–234.
16. Zeviani M, Peterson P, Servidei S, et al. Benign reversible muscle cytochrome c oxidase deficiency: a second case. Neurology 1987; 37:64–67.
17. Servidei S, Bertini E, Vici CD, et al. Benign infantile mitochondrial myopathy due to reversible cytochrome c oxidase deficiency: a third case. Clin Neuropathol 1998;7:209–210.
18. Salo MK, Rapola J, Somer H, et al. Reversible mitochondrial myopathy with cytochrome c oxidase deficiency. Arch Dis Child 1992;67:1033–1035.
19. Suzuki M, Sugie H, Tsurui S, et al. Benign infantile mitochondrial myopathy due to reversible cytochrome c oxidase deficiency: histological and biochemical analysis (in Japanese). No To Hattatsu (Tokyo) 1989;21:543–549.
20. Wada H, Nishio H, Nagaki S, et al. [Benign infantile mitochondrial myopathy caused by reversible cytochrome c oxidase deficiency]. No To Hattatsu (Tokyo) 1996;28:443–447. [Japanese]
21. Horvath R, Kemp JP, Tuppen HAL, et al. Molecular basis of infantile reversible cytocrome c oxidase deficiency myopathy. Brain 2009;132:3165–3174.

22. Muraki K, Nishimura S, Goto Y, et al. The association between haematological manifestation and mtDNA deletions in Pearson syndrome. J Inher Metab Dis 1997;20:697–703.

23. Goto Y, Nishino I, Horai S, Nonaka I. Detection of DNA fragments encompassing the deletion junction of mitochondrial genome. Biochem Biophys Res Commun 1996;222:215–219.

24. Akanuma J, Muraki K, Komaki H, et al. Two pathogenic point mutations exist in the authentic mitochondrial genome, not in the nuclear pseudogene. J Hum Genet 2000;45:337–341.

25. King MP, Attardi G. Human cells lacking mtDNA: repopulation with exogenous mitochondria by complementation. Science 1989; 246:500–503.

26. Yasukawa T, Suzuki T, Suzuki T, et al. Modification defect at anticodon wobble nucleotide of mitochondrial tRNAs Leu (UUR) with pathogenic mutations of mitochondrial myopathy, encephalopathy, lactic acidosis, and stroke-like episodes. J Biol Chem 2000; 275:4251–4257.

27. Varshney U, Lee CP, RajBhandary UL. Direct analysis of aminoacylation levels of tRNAs in vivo. Application to studying recognition of Escherichia coli initiator tRNA mutants by glutaminyl-tRNA synthetase. J Biol Chem 1991;266:24712–24718.

28. Trounce LA, Kim YL, Jun AS, Wallace DC. Assessment of mitochondrial oxidative phosphorylation in patient muscle biopsies, lymphoblasts, and transmitochondrial cell lines. In: Attardi GM, Chomyn A, eds. Methods in enzymology. Vol. 264. San Diego: Academic Press USA, 1996:484–509.

29. Nijtmans LG, Henderson NS, Holt NS. Blue native electrophoresis to study mitochondrial and other protein complexes. Methods 2002;26:327–340.

30. D'Aurelio M, Gajewski CD, Lenaz G, Manfredi G. Respiratory chain supercomplexes set the threshold for respiration defects in human mtDNA mutant cybrids. Hum Mol Genet 2006;15: 19198–19209.

31. Hasegawa H, Matsuoka T, Goto Y, Nonaka I. Strongly succinate dehydrogenase-reactive blood vessels in muscles from patients with mitochondrial myopathy, encephalopathy, lactic acidosis, and stroke-like episodes. Ann Neurol 1991;29:601–605.

32. Jarusalem F, Angelini C, Engel AG, Groover RV. Mitochondrial lipid glycogen (MLG) disease of muscle. A morphologically regressive congenital myopathy. Arch Neurol 1973;29:162–169.

33. Pallanck L, Pak M, Schulman LH. tRNA discrimination in aminoacylation. In: Söll D, RajBhandary U, eds. tRNA: structure, biosynthesis, and function. Washington, DC: American Society for Microbiology, 1995:371–394.

34. Chomyn A, Enrriquez JA, Micol V, et al. The mitochondrial myopathy, encephalopathy, lactic acidosis, and stroke-like episode syndrome-associated human mitochondrial tRNALeu (UUR) mutation causes aminoacylation deficiency and concomitant reduced association of mRNA with ribosomes. J Biol Chem 2000;275: 19198–19209.

35. Yasukawa T, Hino N, Suzuki T, et al. A pathogenic point mutation reduces stability of mitochondrial mutant tRNAIle. Nucleic Acids Res 2000;28:3779–3784.

36. Tritschler HJ, Bonilla E, Lombes A, et al. Differential diagnosis of fatal and benign cytochrome c oxidase-deficient myopathies of infancy: an immunohistochemical approach. Neurology 1991;41: 300–305.

Supplementary Fig 1

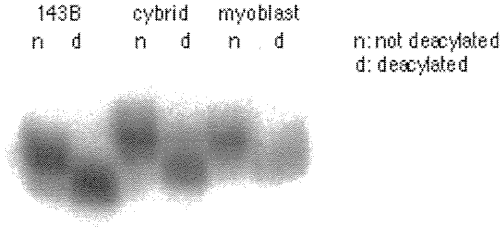

SUPPLEMENTARY INFORMATION

Supplementary Material and Methods

Restriction fragment length polymorphism analysis

To confirm m.14674T>C mutation, the 187-bp PCR fragment with the mismatched and reverse primers was digested by *Bcl I*. If the fragment had m.14674T>C mutation, cleaved fragments of 167 and 20 bps would be obtained. To identify m.14674T>G mutation, we amplified the 541-bp PCR fragment and performed *Nla III* digestion. In the absence of this mutation, cleaved fragments of 408 and 133 bps would be detected; however, if the fragment had m.14674T>G mutation, cleaved fragments of 408 bp would be divided into 242- and 166-bp fragments. Each fragment was detected on a 4% agarose gel and visualized with ethidium bromide under UV light.

Quantification of $tRNA^{Glu}$

Northern blot analysis was performed using total RNA extracted from muscle specimens of patients 2 and 4, from whom a sufficient quantity of RNA was obtained, and from muscle specimens of normal infants (normal controls). Samples of total RNA

were electrophoresed through denaturing 10% polyacrylamide containing 7 M urea. RNA was blotted on a nylon membrane and fixed by UV irradiation. Northern hybridization was then performed using DNA probe specific for mitochondrial tRNA-glutamate ($tRNA^{Glu}$): 5′-ATTCTCGCACGGACTACAACCACGACCAAT-3′ labeled at the 5′ terminus with [γ-^{32}P]ATP (110 TBq/mmol; GE Healthcare Bio-Science, Buckinghamshire, UK). The $tRNA^{Glu}$ amounts were normalized by the amount of mitochondrial tRNA-Leu (UUR) (a probe specific for mitochondrial tRNA-Leu (UUR), 5′-TGTTAAGAAGAGGAATTGAACCTCTGACTG-3′ was used) and nuclear-encoded 5S ribosomal RNA (a probe specific for 5S ribosomal RNA, 5′-GGGTGGTATGGCCGTAGAC-3′ complementary to the 3′ region was used). The DNA probes were labeled at the 5′ terminus with [γ-^{32}P]ATP and T4 polynucleotide kinase (Toyobo, Osaka, Japan). RNAs were quantified by exposing the membrane to an imaging plate on which the radioactivity levels of the bands were measured using a BAS 1000 bioimaging analyzer (Fuji Photo Film, Tokyo, Japan).

Acid polyacrylamide gel electrophoresis analysis

Total RNA samples extracted from cybrids derived from fibroblasts of patient 6

and human osteosarcoma 143B cells (normal control) were prepared under acidic conditions in a cold room and then dissolved in 0.1 M NaOAc (pH 5.0) according to the literature to prevent deacylation [26]. A portion of RNA samples was incubated in a buffer containing 50 mM Tris-HCl (pH 9.5) for complete deacylation of tRNA samples. The same amount of total RNA containing aminoacyl-tRNAs or forcibly deacylated tRNAs in an acid-loading solution were electrophoresed to separate aminoacyl-$tRNA^{Glu}$ and uncharged $tRNA^{Glu}$. RNA was then analyzed by Northern hybridization using the probe specific for mitochondrial $tRNA^{Glu}$:

5′-ATTCTCGCACGGACTACAACCACGACCAAT-3′ labeled at the 5′ terminus with [γ-^{32}P]ATP. The DNA probes were labeled at the 5′ terminus with [γ-^{32}P]ATP and T4 polynucleotide kinase. RNAs were quantified by exposing the membrane to an imaging plate on which the radioactivity levels of the bands were measured using a BAS 1000 bioimaging analyzer.

Acta Neuropathol (2010) 119:481–486
DOI 10.1007/s00401-010-0660-7

ORIGINAL PAPER

Congenital myotonic dystrophy can show congenital fiber type disproportion pathology

Kayo Tominaga · Yukiko K. Hayashi · Kanako Goto · Narihiro Minami · Satoru Noguchi · Ikuya Nonaka · Tetsuro Miki · Ichizo Nishino

Received: 19 November 2009 / Revised: 15 February 2010 / Accepted: 15 February 2010 / Published online: 24 February 2010

Abstract Congenital myotonic dystrophy (CDM) is associated with markedly expanded CTG repeats in *DMPK*. The presence of numerous immature fibers with peripheral halo is a characteristic feature of CDM muscles together with hypotrophy of type 1 fibers. Smaller type 1 fibers with no structural abnormality are a definitive criterion of congenital fiber type disproportion (CFTD). Nonetheless, we recently came across a patient who was genetically confirmed as CDM, but had been earlier diagnosed as CFTD when he was an infant. In this study, we performed clinical, pathological, and genetic analyses in infantile patients pathologically diagnosed as CFTD to evaluate CDM patients indistinguishable from CFTD. We examined CTG repeat expansion in *DMPK* in 28 infantile patients pathologically diagnosed as CFTD. Mutation screening of *ACTA1* and *TPM3* was performed, and we compared clinical and pathological findings of 20 CDM patients with those of the other cohorts. We identified four (14%) patients with CTG expansion in *DMPK*. *ACTA1* mutation was identified in four (14%), and *TPM3* mutation was found in two (7%) patients. Fiber size disproportion was more prominent in patients with *ACTA1* or *TPM3* mutations as compared to CFTD patients with CTG expansion. A further three patients among 20 CDM patients showed pathological findings similar to CFTD. From our results, CDM should be excluded in CFTD patients.

Keywords Congenital myotonic dystrophy (CDM) · Congenital fiber type disproportion (CFTD) · *DMPK* · CTG expansion · *ACTA1* · *TPM3*

Introduction

Congenital myotonic dystrophy (CDM; OMIM 160900) is caused by marked expansion of trinucleotide (CTG) repeat in the 3′ untranslated region of the dystrophia myotonica protein kinase gene (*DMPK*; OMIM 605377) on chromosome 19q [1, 5, 9]. The CTG repeat in normal individuals varies from 5 to 35, whereas it expands to more than 1,000 repeats in CDM [7]. Typically, the mothers of CDM patients show clinical features of myotonic dystrophy which makes the diagnosis of CDM easier. Clinically, CDM patients show hypotrophy at birth, tented upper lip, facial muscle weakness, and neonatal respiratory insufficiency. Mental retardation becomes evident in later life. On muscle pathology, the presence of numerous immature fibers with peripheral halo is a characteristic feature together with increased number of fibers with centrally placed nuclei and hypotrophy of type 1 fibers, mimicking myotubular myopathy [6].

Smaller sized type 1 fibers as compared to type 2 fibers are a characteristic pathological feature of congenital fiber type disproportion (CFTD; OMIM 255310). CFTD is a

Electronic supplementary material The online version of this article (doi:10.1007/s00401-010-0660-7) contains supplementary material, which is available to authorized users.

K. Tominaga · Y. K. Hayashi · K. Goto · N. Minami · S. Noguchi · I. Nonaka · I. Nishino (✉)
Department of Neuromuscular Research, National Institute of Neuroscience, National Center of Neurology and Psychiatry, 4-1-1 Ogawa-higashi, Kodaira, Tokyo 187-8502, Japan
e-mail: nishino@ncnp.go.jp

T. Miki
Proteo-Medicine Research Center, Ehime University, Toon, Ehime 791-0295, Japan

K. Tominaga · T. Miki
Department of Geriatric Medicine, Ehime University Graduate School of Medicine, Toon, Ehime 791-0295, Japan

congenital myopathy defined by type 1 fiber hypotrophy of 12% or more than type 2 fibers, and with the absence of structural abnormalities within myofibers [2]. Type 1 fiber predominance is also commonly seen. Clinically, CFTD patients show hypotonia, facial muscle weakness, and severe respiratory insufficiency at birth. Long face, high-arched palate, and joint contractures are often seen. CFTD is a genetically heterogeneous disorder and mutations in the genes for tropomyosin 3 (*TPM3*; OMIM 191030), α-skeletal muscle actin 1 (*ACTA1*; OMIM 102610), and selenoprotein N1 (*SEPN1*; OMIM 606210) have been identified [3, 4, 8]. Reportedly *TPM3* mutations are the most common ones and observed approximately in 20–25% of the CFTD patients [4]. *ACTA1* mutations were identified in 6% of CFTD [8], and only one family was reported having an *SEPN1* mutation [3].

Although the muscle pathology features of CDM seem to be well defined, our experience with one CDM patient who was previously diagnosed as CFTD made us hypothesize that CDM may have features other than the presently defined ones, both in terms of muscle pathology and clinical characteristics. In this study, we looked for CDM patients among patients who presented with CFTD. We also performed clinical and pathological analysis to find out whether patients with CDM can be distinguished from CFTD.

Materials and methods

Patients

All clinical materials used in this study were obtained for diagnostic purposes and with informed consent. This work was approved by the Ethical Committee of National Center of Neurology and Psychiatry (NCNP). In this study, we chose muscle specimens from patients younger than 1 year of age. From the muscle repository of NCNP, there were 28 unrelated patients who were pathologically diagnosed as CFTD. Twenty CDM patients, who had symptomatic family members and whose diagnosis was genetically confirmed, were also used for comparison.

Histochemistry

Biopsied skeletal muscles were frozen with isopentane cooled in liquid nitrogen. Serial frozen sections of 10 μm thickness were stained with hematoxylin and eosin (H & E), modified Gomori-trichrome (mGT), NADH-tetrazolium reductase (NADH-TR), and ATPases (pH 10.6, pH 4.6 and pH 4.3). For each muscle specimen, the mean fiber diameter was determined by obtaining the shortest anteroposterior diameter of 100 each of type 1 and type 2 (A + B) fibers using ATPase stains. The myofiber diameter was used to calculate the fiber size disproportion (FSD). FSD was computed as: difference of type 2 fiber diameter (mean) and type 1 fiber diameter (mean) divided by type 2 fiber diameter (mean) × 100%.

Genetic analyses

Genomic DNA was extracted from peripheral lymphocytes or frozen muscle specimens using standard protocol. To examine CTG repeat expansion in *DMPK*, triplet repeat primed PCR was performed as described previously [12]. The presence of the expanded CTG repeats was examined by Gene Mapper using ABI PRISM 310 automated sequencer (Applied Biosystems Japan Co., Ltd, Japan). To know the approximate number of triplet repeats, we performed Southern blotting analysis using PCR-amplified CTG repeats because of the limited amounts of muscle specimens [10]. The primer sequences used in this study are F: 5′-CGAACGGGGCTCGAAGGGTCCTTGTAGC CG-3′, and R: 5′-TCTTTCTTTACCAGACACTAGGG-3′.

The PCR products were electrophoresed with 1% of Seakem HGT agarose gel (Cambrex Bio Science Rockland Inc., ME, USA), transferred to Hybond-XL (GE Healthcare, UK) for overnight, hybridized with ^{32}P-labeled probes of $(CTG)_{10}$ oligonucleotide at 65°C for overnight, and detected using BAS2500 (Fuji Film, Japan). By using genomic DNA from a CDM patient with known CTG repeat number, we confirmed that this PCR-based method can detect the corresponding size of the CTG repeats using genomic DNA. For mutation screening of *ACTA1* and *TPM3*, all exons and their flanking intronic regions were amplified by PCR and directly sequenced by an ABI PRISM 3100 automated sequencer (Applied Biosystems). Primer sequences are listed in the Supplemental Table.

Statistical analyses

All data are presented as means ± SD. Comparisons among groups were done by using Student's *t* test and analysis of variance (ANOVA) as appropriate. Statistical significance was considered when p value was less than 0.05.

Results

Genetic analyses

By using triplet repeat primed PCR, expanded CTG repeats in *DMPK* were detected in 4 of 28 (14%) unrelated patients who were pathologically diagnosed as CFTD (Figs. 1, 2a). This diagnosis of CDM was further confirmed by Southern

blotting analysis, wherein all four patients had more than 1,000 CTG repeats (Fig. 2b). We also identified three heterozygous *ACTA1* mutations (p.Gly48Cys, p.Leu221-Pro, and p.Pro332Ser) in four unrelated CFTD patients. Two mutations of p.Leu221Pro and p.Pro332Ser have already been reported [8], whereas the p.Gly48Cys mutation observed in two patients was a novel one. The Gly48 is a highly conserved amino acid among several species. Two unrelated CFTD patients had the same heterozygous mutation p.Arg168Cys in *TPM3*, which was previously reported in CFTD patients [4].

Clinical findings

We compared the clinical findings among 4 CFTD patients with CTG expansion and 6 CFTD patients with *ACTA1* or *TPM3* mutations, and compared the clinical features with 20 patients genetically confirmed as CDM (Table 1). In terms of family history, none of the four CFTD patients with CTG expansion had a positive family history. This is in stark contrast with the typical picture in CDM patients, as all of them had at least one symptomatic family member. Hydramnios and premature delivery were seen in more than 50% of the CFTD patients with CTG expansion and CDM, but none of CFTD patients with *ACTA1* or *TPM3* mutations. Hypotonia and respiratory insufficiency at birth were seen in all groups except for two patients with *TPM3* mutation.

Muscle pathological findings

As muscle pathology can have drastic changes according to the gestational age of infantile patients, we adjusted the age by setting the full-term day (37 weeks of gestation) as putative birthday. After adjustment, the age at biopsy of the CDM patients ranged from −7 to 43 weeks, and those of the four CFTD patients with CTG expansion were from 21 to 42 weeks.

Congenital fiber type disproportion is defined as a congenital myopathy wherein FSD is higher than 12%, but with no associated structural abnormalities within the myofibers [2]. In this study, FSD in CDM, CFTD with CTG expansion, CFTD with *ACTA1* mutation, and CFTD with *TPM3* mutation was calculated to be 7.2 ± 6.8% (mean ± SD), 23.0 ± 5.0, 47.5 ± 4.0, and 52.0 ± 9.9%, respectively (Fig. 3). FSD was significantly ($p < 0.05$) higher in CFTD with *ACTA1* or *TPM3* mutations as compared to the CFTD patients with CTG expansion and CDM.

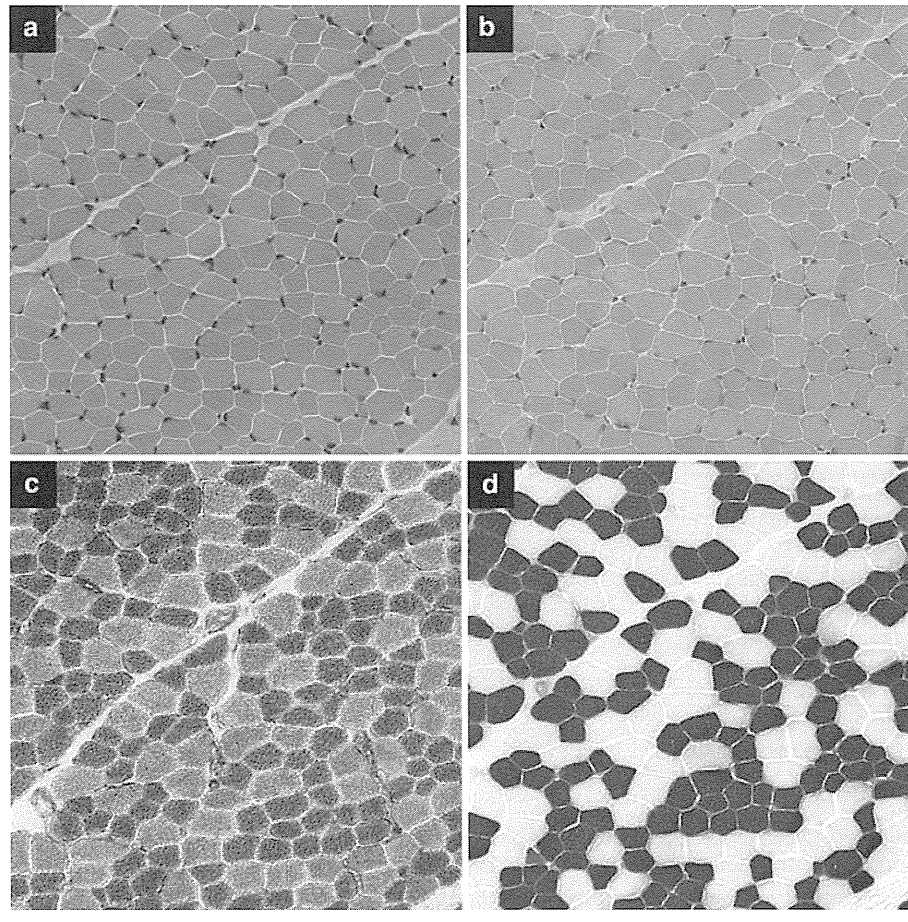

Fig. 1 Muscle pathology of a 42-week-old CFTD patient with CTG expansion. **a** Hematoxylin and eosin, **b** modified Gomori trichrome, **c** NADH-TR, and **d** ATPase (pH 4.4) stain. Type 1 fiber atrophy (FSD [(mean type 2 fiber diameter) − (mean type 1 fiber diameter)/mean type 2 fiber diameter × 100] = 26%), type 1 fiber predominance (65%), and only 1% of type 2C fibers with no peripheral halo is seen. *Bar* 50 μm

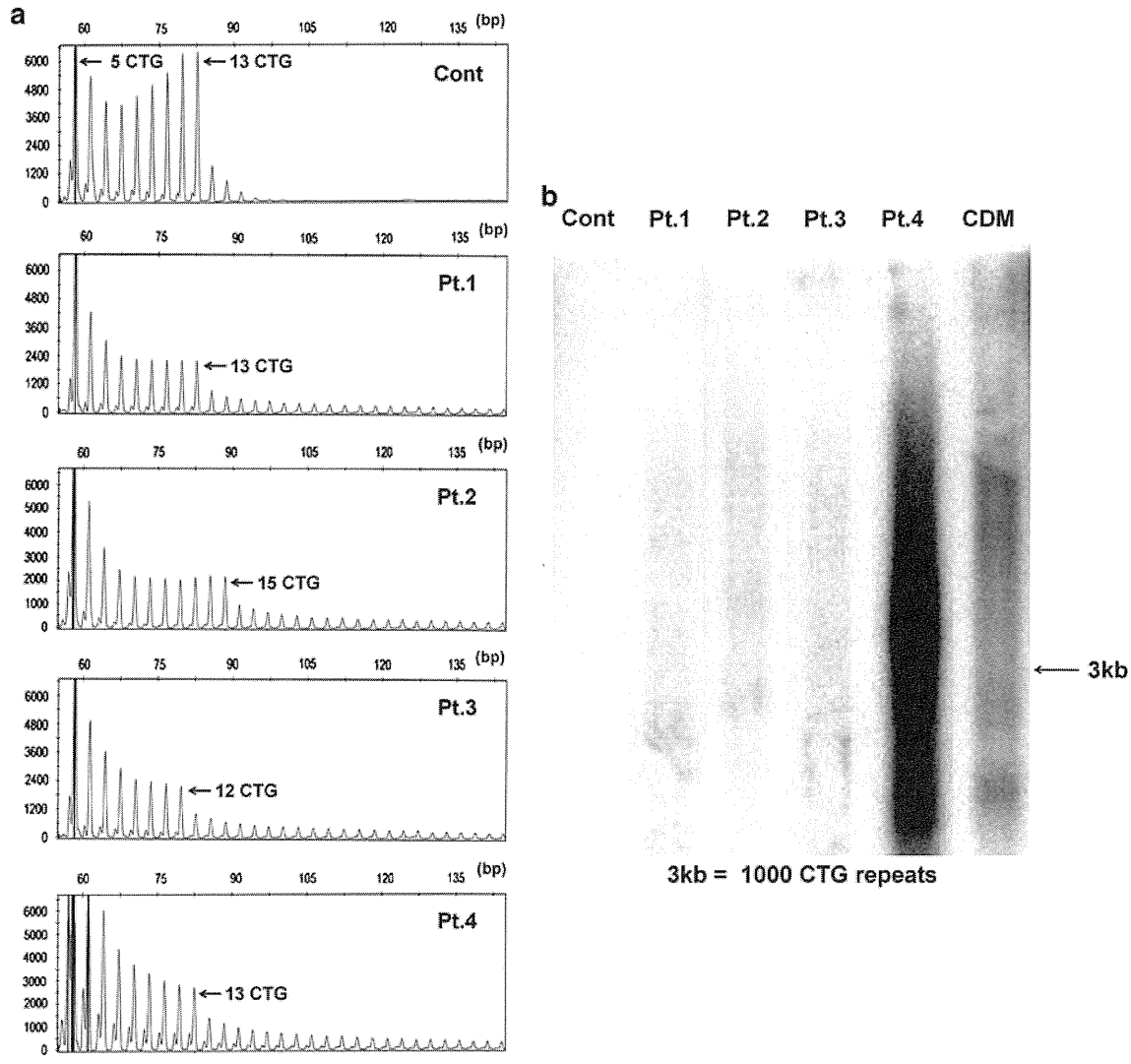

Fig. 2 Genetic analyses. **a** Triplet repeat primed PCR. Control (*Cont*) has 5 and 13 CTG repeats. The four CFTD patients (Pt.1, Pt.2, Pt.3, and Pt.4) have the ladder pattern that represents a large CTG allele together with higher peaks that show normal-sized allele (*arrows*). **b** Southern blotting analysis using PCR products. Four CFTD patients (Pt.1, Pt.2, Pt.3, and Pt.4) and one genetically confirmed CDM showed smear band larger than 3 kb corresponding to 1,000 CTG repeats, whereas a control (*Cont*) has no detectable band

Table 1 Clinical summary of the patients

Pathological diagnosis	CDM	CFTD	CFTD	CFTD
Gene mutation	CTG expansions in *DMPK*	CTG expansions in *DMPK*	*ACTA1*	*TPM3*
Number of patients	20	4	4	2
Hydramnios	65% (13/20)	50% (2/4)	0% (0/4)	0% (0/2)
Premature delivery (<37w)	50% (10/20)	50% (2/4)	0% (0/4)	0% (0/2)
Hypotonia at birth	100% (20/20)	100% (4/4)	100% (4/4)	0% (0/2)
Respiratory insufficiency at birth	95% (19/20)	75% (3/4)	75% (3/4)	0% (0/2)
Symptoms seen in family	100% (20/20)	0% (0/4)	0% (0/4)	0% (0/2)

In addition to FSD, we also checked other features in pathology that define either CFTD or CDM. Type 1 fiber predominance is a notable pathological finding observed in CFTD, and all our CFTD patients, including those with CTG expansion, showed type 1 fiber predominance. The mean composition of type 1 fibers in CDM, CFTD with

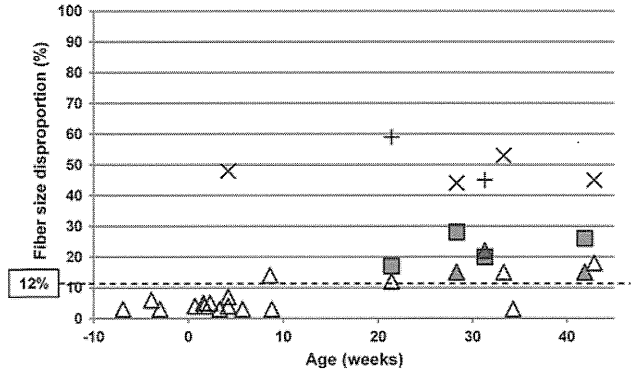

Fig. 3 Fiber size disproportion (*FSD*) of each patient. CFTD with CTG expansion (*filled square*; $N = 4$), CDM (*open triangle*; $N = 17$), CDM with similar pathological findings to CFTD (*filled triangle*; $N = 3$), CFTD with *ACTA1* mutations (*multi symbol*; $N = 4$), and CFTD with *TPM3* mutations (*plus*; $N = 2$). *Dot line* at 12% of FSD is the lowest FSD by the definition of CFTD

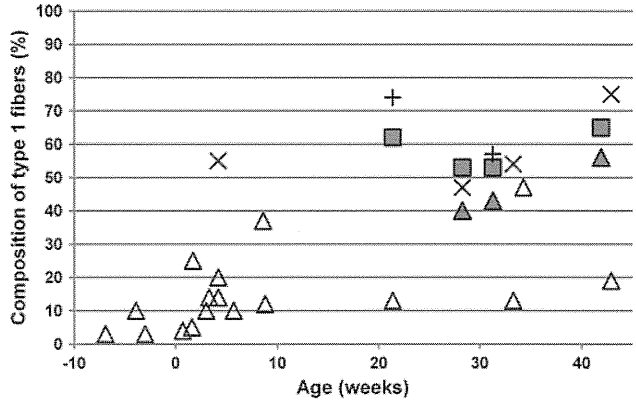

Fig. 4 Composition of type 1 fibers in each patient. *Filled square* CFTD with CTG expansion, *open triangle* CDM, *filled triangle* CDM with similar pathological findings to CFTD, *multi symbol* CFTD with *ACTA1* mutations, and *plus* CFTD with *TPM3* mutations

CTG expansion, and CFTD with *ACTA1* or *TPM3* mutations was 19.6 ± 16.3, 58.2 ± 6.2, 57.8 ± 2.0, and 65.5 ± 12.0%, respectively (Fig. 4). On the other hand, the presence of numerous immature type 2C fibers with peripheral halo is a characteristic finding in CDM. A markedly increased number of type 2C fibers were actually observed in CDM especially in patients younger than 10 weeks of adjusted age (Fig. 5). The frequency of type 2C fibers was inversely correlated to age of patients, while the number of type 1 fibers was directly proportional to age of patients. In other words, type 2C fibers were increased among younger age, while type 1 fiber predominance is seen more among older patients. Peripheral halo was observed in 14 of 20 (70%) CDM patients even in a 43-week-old patient. In CFTD patients with CTG expansion, type 2C fibers accounted for less than 20% and in CFTD with *ACTA1* or *TPM3* mutations, only a few type 2C fibers were seen. No peripheral halo was seen in either group. The increased number of fibers with internally located nuclei is another characteristic pathological finding of myotonic dystrophy. In our series, fibers containing internal nuclei were variably increased up to 26% in CDM patients, whereas less than 2% of fibers contained internal nuclei in the CFTD patients with CTG expansion or mutation in *ACTA1* or *TPM3*. The number of the fibers with internal nuclei is relatively correlated to the number of immature fibers in CDM, which may reflect immaturity of the fibers as described previously [6, 11].

Of the 20 CDM patients, 3 showed pathological findings similar to CFTD with CTG expansion. The ages of these three patients were 29, 32 and 42 weeks, respectively. FSD was 15–21%, with less than 20% of type 2C fibers and no peripheral halo. In these patients, the clinical diagnosis of CDM was made based upon the presence of the symptomatic family member.

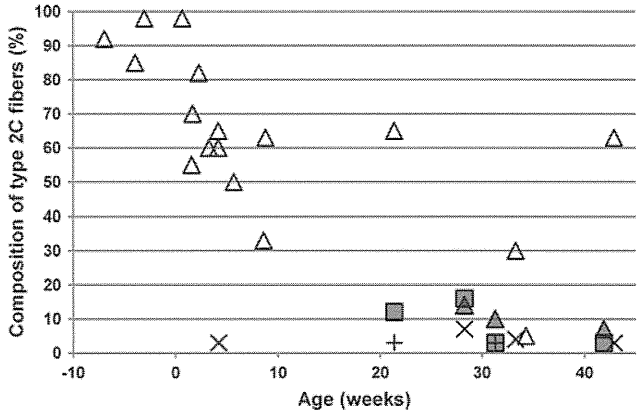

Fig. 5 Composition of type 2C fibers in each patient. *Filled square* CFTD with CTG expansion, *open triangle* CDM, *filled triangle* CDM with similar pathological findings to CFTD, *multi symbol* CFTD with *ACTA1* mutations, and *plus* CFTD with *TPM3* mutations

Discussion

In this study, we identified 4 of 28 patients (14%) who have CTG expansion in *DMPK* but were pathologically diagnosed as CFTD. Clinical symptoms of CFTD and CDM are quite similar during neonatal stage, including hypotonia and respiratory insufficiency. However, most of CDM patients are readily diagnosed by the presence of symptomatic family members, typically the mother. In fact, all CDM patients in our series had symptomatic family members and 75% of the mothers had the diagnosis of myotonic dystrophy. In contrast, no notable clinical symptoms were recorded in the mother of the CFTD patients with CTG expansion, and we could not examine the repeat size of the mothers. No marked difference in the size of CTG repeats was seen between CFTD patients with CTG expansion and CDM.

Among the CDM patients we examined, three patients showed pathological findings similar to those observed in CFTD with CTG expansion. They showed a small number of type 2C fibers, no peripheral halo, and hypotrophy of type 1 fibers (FSD >15%). The diagnosis of CDM was done from the typical clinical symptoms of myotonic dystrophy observed in the family member. Interestingly the ages of these three patients were over 29 weeks. Consistently, the ages of the patients who have CFTD with CTG expansion ranged from 21 to 42 weeks. These results suggest that CFTD pathology may be seen in this age range of CDM patients.

We identified four patients with mutations in *ACTA1* and two in *TPM3*. FSD in these patients was over 45% and significantly higher than that observed in CFTD with CTG expansion. This finding is also consistent with a previous report of CFTD patients with *TPM3* mutations whose muscle showed higher than 50% of FSD [4]. From these results, CDM should be considered for the patients whose muscle shows CFTD with FSD lower than 40%. In our series, only 4 (14%) and 2 (7%) of 28 patients had the mutations respectively in *ACTA1* and *TPM3*, leaving 18 (65%) patients still genetically uncharacterized and suggesting that defects in these genes may not be the major causes of CFTD in Japan. Further studies are necessary to elucidate such causes.

Acknowledgments We thank Dr. May Christine V. Malicdan (National Institute of Neuroscience, NCNP) for reviewing the manuscript. This study was supported by: the a Grant-in-Aid for Scientific Research and a Grain-in-aid for Exploratory Research from Japan Society for the Promotion of Science; by Research on Psychiatric and Neurological Diseases and Mental Health of Health Labour Sciences Research Grant and the Research Grant (20B-12, 20B-13) for Nervous and Mental Disorders from the Ministry of Health, Labour, and Welfare; by Research on Health Sciences focusing on Drug Innovation from the Japanese Health Sciences Foundation; and by the Program for Promotion of Fundamental Studies in Health Sciences of the National Institute of Biomedical Innovation (NIBIO).

References

1. Brook JD, McCurrach ME, Harley HG et al (1992) Molecular basis of myotonic dystrophy: expansion of a trinucleotide (CTG) repeat at the 3′ end of a transcript encoding a protein kinase family member. Cell 69:385
2. Clarke NF, North KN (2003) Congenital fiber type disproportion—30 years on. J Neuropathol Exp Neurol 62:977–989
3. Clarke NF, Kidson W, Quijano-Roy S et al (2006) SEPN1: associated with congenital fiber-type disproportion and insulin resistance. Ann Neurol 59:546–552
4. Clarke NF, Kolski H, Dye DE et al (2008) Mutations in TPM3 are a common cause of congenital fiber type disproportion. Ann Neurol 63:329–337
5. Fu YH, Pizzuti A, Fenwick RG Jr et al (1992) An unstable triplet repeat in a gene related to myotonic muscular dystrophy. Science 255:1256–1258
6. Harper PS, Monckton DG (2004) Myotonic dystrophy. In: Engel AG, Franzini-Armstrong C (eds) Myology, 3rd edn. McGraw-Hill, New York, pp 1039–1076
7. The International Myotonic Dystrophy Consortium (IDMC) (2000) New nomenclature and DNA testing guidelines for myotonic dystrophy type 1 (DM1). Neurology 54:1218–1221
8. Laing NG, Clarke NF, Dye DE et al (2004) Actin mutations are one cause of congenital fibre type disproportion. Ann Neurol 56:689–694
9. Mahadevan M, Tsilfidis C, Sabourin L et al (1992) Myotonic dystrophy mutation: an unstable CTG repeat in the 3′ untranslated region of the gene. Science 255:1253–1255
10. Surh LC, Mahadevan M, Korneluk RG (1998) Analysis of trinucleotide repeats in myotonic dystrophy. In: Dracopoli NC, Haines JL, Korf BR, Morton CC et al (eds) Current protocols in human genetics, vol 2. Wiley, New York, unit 9.6.1-13
11. Tanabe Y, Nonaka I (1987) Congenital myotonic dystrophy. Changes in muscle pathology with ageing. J Neurol Sci 77:59–68
12. Warner JP, Barron LH, Goudie D et al (1996) A general method for the detection of large CAG repeat expansions by fluorescent PCR. J Med Genet 33:1022–1026

Specific phosphorylation of Ser458 of A-type lamins in *LMNA*-associated myopathy patients

Hiroaki Mitsuhashi[1], Yukiko K. Hayashi[1,*], Chie Matsuda[2], Satoru Noguchi[1], Shuji Wakatsuki[3], Toshiyuki Araki[3] and Ichizo Nishino[1]

[1]Department of Neuromuscular Research, National Institute of Neuroscience, National Center of Neurology and Psychiatry, 4-1-1 Ogawa-higashi, Kodaira, Tokyo 187-8502, Japan
[2]Neuroscience Research Institute, AIST, Central 6, Tsukuba, Ibaraki 305-8566, Japan
[3]Department of Peripheral Nervous System Research, National Institute of Neuroscience, National Center of Neurology and Psychiatry, Kodaira, Tokyo 187-8502, Japan
*Author for correspondence (hayasi_y@ncnp.go.jp

Accepted 9 August 2010
Journal of Cell Science 123, 3893-3900

doi:10.1242/jcs.072157

Summary

Mutations in *LMNA*, which encodes A-type nuclear lamins, cause various human diseases, including myopathy, cardiomyopathy, lipodystrophy and progeria syndrome. To date, little is known about how mutations in a single gene cause a wide variety of diseases. Here, by characterizing an antibody that specifically recognizes the phosphorylation of Ser458 of A-type lamins, we uncover findings that might contribute to our understanding of laminopathies. This antibody only reacts with nuclei in muscle biopsies from myopathy patients with mutations in the Ig-fold motif of A-type lamins. Ser458 phosphorylation is not seen in muscles from control patients or patients with any other neuromuscular diseases. In vitro analysis confirmed that only lamin A mutants associated with myopathy induce phosphorylation of Ser458, whereas lipodystrophy- or progeria-associated mutants do not. We also found that Akt1 directly phosphorylates Ser458 of lamin A with myopathy-related mutations in vitro. These results suggest that Ser458 phosphorylation of A-type lamins correlates with striated muscle laminopathies; this might be useful for the early diagnosis of *LMNA*-associated myopathies. We propose that disease-specific phosphorylation of A-type lamins by Akt1 contributes to myopathy caused by *LMNA* mutations.

Key words: Laminopathy, A-type lamins, EDMD, LGMD1B, Akt

Introduction

Mutations in *LMNA* cause at least 13 human hereditary diseases, collectively termed 'laminopathies'. These include striated muscle diseases, such as autosomal dominant and recessive forms of Emery-Dreifuss muscular dystrophy (AD/AR-EDMD) (Bonne et al., 1999; Raffaele Di Barletta et al., 2000), limb-girdle muscular dystrophy type 1B (LGMD1B) (Muchir et al., 2000), *LMNA*-related congenital muscular dystrophy (L-CMD) (Quijano-Roy et al., 2008) and dilated cardiomyopathy (Fatkin et al., 1999), and other conditions including Hutchinson-Gilford progeria syndrome (HGPS) (De Sandre-Giovannoli et al., 2003; Eriksson et al., 2003), atypical Werner syndrome (Chen et al., 2003), mandibuloacral dysplasia (MAD) (Novelli et al., 2002) and Dunnigan-type familial partial lipodystrophy (FPLD) (Shackleton et al., 2000). It is still not clear how mutations in *LMNA* cause such a wide variety of tissue-specific degenerative diseases, although A-type lamins are ubiquitously expressed.

A-type lamins, of which lamin A and lamin C are the predominant somatic cell isoforms, are type V intermediate filament proteins that form the nuclear lamina, a meshwork on the nucleoplasmic side of the inner nuclear membrane (Burke and Stewart, 2002; Capell and Collins, 2006). Like all intermediate filament proteins, lamins have a tripartite structure consisting of an N-terminal head, a central coiled-coil rod domain and a large globular C-terminal tail. The C-terminal tail domain has an immunoglobulin-like fold (Ig-fold) motif (residues 436–544); these motifs are known to be involved in protein–protein interactions (Dechat et al., 2000; Lee et al., 2001; Sakaki et al., 2001; Zastrow et al., 2006; Zastrow et al., 2004). In addition to their primary role in providing mechanical support for nuclear membranes to maintain nuclear shape and size (Goldman et al., 2004), lamin filaments are believed to play important roles in mitosis (Tsai et al., 2006), chromatin organization (Glass et al., 1993; Park et al., 2009; Taniura et al., 1995), transcription (Spann et al., 2002) and DNA replication (Moir et al., 2000; Spann et al., 1997).

According to the PhosphoSite database (http://www.phosphosite.org/), more than 30 phosphorylation sites in human A-type lamins have been reported. Phosphorylation of Thr19, Ser22 and Ser392 leads to depolymerization of lamin filaments during nuclear envelope breakdown in mitosis and meiosis (Haas and Jost, 1993; Heald and McKeon, 1990; Peter et al., 1990; Ward and Kirschner, 1990), but the physiological importance of the phosphorylation of other sites in A-type lamins is largely unknown. Previously, Cenni et al. reported that N-terminal phosphorylation of lamin A was specifically decreased in the muscles of four AD-EDMD or LGMD1B patients (Cenni et al., 2005), implicating unidentified lamin A phosphorylation sites in the pathomechanism of AD-EDMD and LGMD1B.

Here, we produced site- and phosphorylation-state-specific antibodies against human A-type lamins, and found that the antibody against phosphorylated Ser458 specifically detects myopathy patients who have mutations within the Ig-fold motif of the C-terminal tail domain of A-type lamins. In vitro expression analysis revealed that Ser458 phosphorylation was specific to myopathy-causing *LMNA* mutations, because it was not detected in cells with mutations related to FPLD or progeria. These results imply that Ser458 phosphorylation might have particular roles in the pathomechanism of *LMNA*-associated myopathy.

Results

Ser458 phosphorylation of A-type lamins in the muscles of *LMNA*-associated myopathy patients

To examine the phosphorylation state of A-type lamins, we raised rabbit polyclonal antibodies against three phosphorylated A-type lamin peptides – Ser5-*P*, Thr416-*P* and Ser458-*P* (Fig. 1A); these serine and threonine residues are well conserved between species. We performed immunohistochemistry of muscle specimens from 17 genetically confirmed *LMNA*-associated myopathy patients, including AD-EDMD, LGMD1B and L-CMD patients.

Using the purified anti-phospho-Ser458 antibody (anti-Ser458-*P* Ab), we found clear nuclear staining in muscles from patients with *LMNA*-associated myopathies, but not in control muscles (Fig. 1Ba–d). Notably, strong immunoreaction to anti-Ser458-*P* Ab was observed in all eight patients carrying a mutation within the Ig-fold motif, whereas the remaining nine patients with mutations outside of the Ig-fold domain showed barely detectable nuclear staining (Table 1). Ser458 is an evolutionarily highly conserved residue within the Ig-fold motif (amino acids 436–544) of A-type lamins (supplementary material Fig. S1A). Anti-Ser458-*P* Ab staining was independent of patient age and sex, and independent of the nature or severity of myopathy, because positive staining for Ser458-*P* was seen in AD-EDMD, LGMD1B, L-CMD and infantile inflammatory myopathy (IIM) cases.

Positive staining with the anti-Ser458-*P* antibody was detected in myonuclei [both peripheral and centrally located (Fig. 1Bb,d,e,g)], vascular endothelial and smooth muscle cell nuclei (Fig. 1Bi), and the nuclei of unidentified cells outside the basal lamina (Fig. 1Bf,h). Double staining with anti-Ser458-*P* and anti-Pax7 antibodies also revealed positive staining in nuclei of satellite cells in patient muscles (Fig. 1Bj–l). Double staining with antibodies for Ser458-*P* and pan-A-type lamins showed that 69.0±7.3% of nuclei were immunostained in patient muscles with mutations in the Ig-fold domain. These results suggest that the Ser458 phosphorylation might be common in *LMNA*-associated myopathy patients with mutations in the Ig-fold domain of A-type lamins.

Consistent with the immunohistochemistry results, the anti-Ser458-*P* Ab detected two main bands at 70 kDa and 65 kDa, corresponding to lamins A and C, respectively, in muscle from laminopathy patients, but not in unaffected control muscle (Fig. 2).

No Ser458 phosphorylation of A-type lamins in patients with other neuromuscular disorders

To determine whether Ser458 phosphorylation is specific to *LMNA*-associated myopathy, we immunostained muscle specimens from patients with other neuromuscular diseases, including X-linked EDMD (X-EDMD (Fig. 3c,d), Duchenne muscular dystrophy (DMD) (Fig. 3e,f), Becker muscular dystrophy (BMD) (Fig. 3g,h), LGMD2A (Fig. 3i,j), LGMD2B (Fig. 3k,l), sporadic inclusion body myositis (sIBM) (Fig. 3,m,n), idiopathic polymyositis (PM) (Fig. 3o,p) and myotonic dystrophy type 1 (MyD1) (Fig. 3q,r). As shown in Fig. 3, Ser458 phosphorylation was only observed in

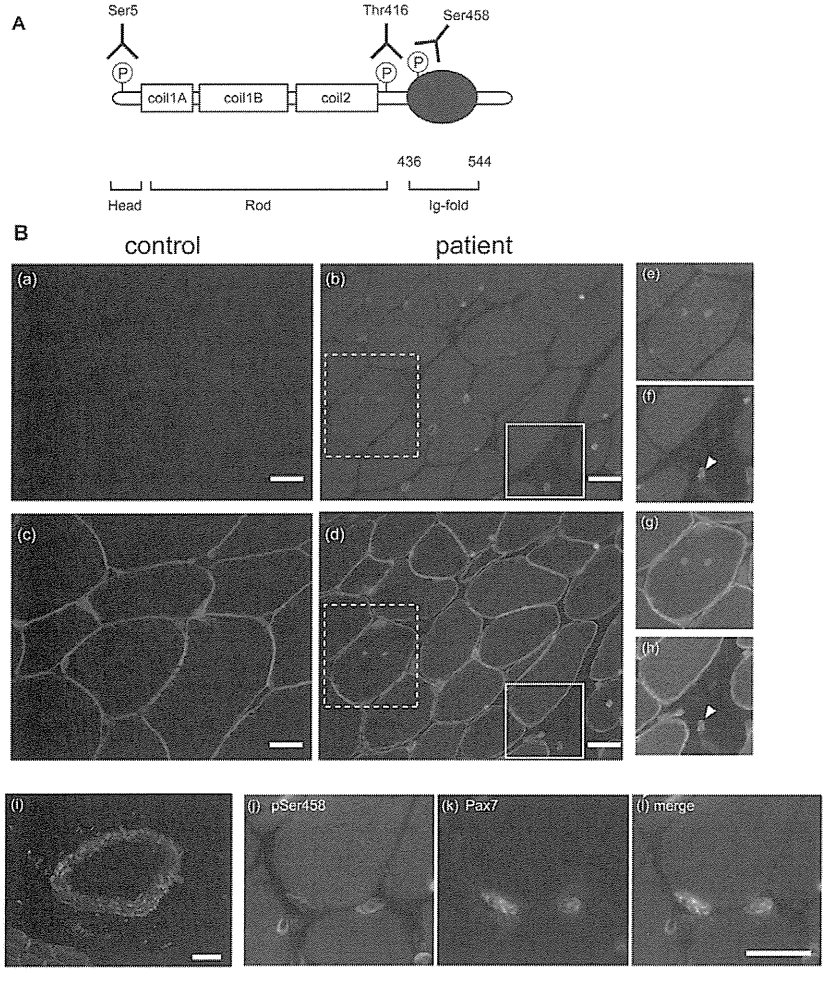

Fig. 1. Ser458 of A-type lamins is specifically phosphorylated in muscles from *LMNA*-associated myopathy patients. (**A**) Schematic model of three antibodies against phosphorylated A-type lamins (Ser5-*P* Ab, Thr416-*P* Ab and Ser458-*P* Ab). Amino acid residues 436–544 form an Ig-fold structure in the C-terminal globular tail domain. (**B**) Immunohistochemistry of human muscles with anti-Ser458-*P* antibody. Nuclei in patient muscle (P11) show positive staining for anti-Ser458-*P* antibody (b,d), whereas no positive nuclear staining is seen in control muscle (a,c). Anti-Ser458-*P* Ab is green and anti-merosin antibody is red. (c,d) Merged images. Blue is DAPI staining. (e,f) Magnified images of boxes in b. (g,h) Magnified images of boxes in d. Note that centrally placed nuclei and nuclei in non-muscle cells outside of the basal lamina (arrowheads) are immunostained with anti-Ser458-*P* Ab. (i) Nuclei in blood vessels in the patient muscle (P14) are also immunostained with anti-Ser458-*P* Ab. (j–l) Double staining of *LMNA*-associated myopathy patient muscle (P12) with anti-Ser458-*P* Ab (j) and anti-pax7 (k) reveals colocalization (l), indicating the occurrence of Ser458 phosphorylation in the patient satellite cells. Scale bars: 20 μm.